12-1991

Remote estimation of the diffuse attenuation coefficient in a moderately turbid estuary

Richard P. Stumpf
U.S.G.S.

Jonathan Pennock
University of New Hampshire - Main Campus

Recommended Citation
Stumpf, R. P. and J. R. Pennock. 1991. Remote estimation of the diffuse attenuation coefficient in a moderately turbid estuary. Remote Sensing of Environment 38:183-191.

REMOTE SENS. ENVIRON. 38:183–191 (1991)

Remote Estimation of the Diffuse Attenuation Coefficient in a Moderately Turbid Estuary

Richard P. Stumpf

U. S. Geological Survey, Center for Coastal Geology and Regional Marine Studies, St. Petersburg

Jonathan R. Pennock

University of Alabama, Marine Environmental Sciences Consortium, Dauphin Island

Solutions of the radiative transfer equation are used to derive relationships of water reflectance to the diffuse attenuation coefficient (K) in moderately turbid water ($K > 0.5\ m^{-1}$). Data sets collected from the NOAA AVHRR and in situ *observations from five different dates confirm the appropriateness of these relationships, in particular the logistic equation. Values of K calculated from the reflectance data agree to within 60% of the observed values, although the reflectance derived using a more comprehensive aerosol correction is sensitive to chlorophyll concentrations greater than 50 $\mu g\ L^{-1}$. Agreement between* in situ *and remote observations improves as the time interval between samples is narrowed.*

INTRODUCTION

Light availability is a critical regulator of estuarine primary production both for phytoplankton (Pennock and Sharp, 1986) and for seagrasses (Orth and Moore, 1983). As a result, both basic and management-related research efforts require information on the availability of light in estuarine waters. Of particular interest is the measurement of the diffuse attenuation coefficient, which defines the presence of light versus depth, the depth of the euphotic zone, and ultimately the maximum depth of primary production.

Interest in water clarity and quality have lead to efforts to relate remote observations from satellite or airborne sensors to *in situ* light and optical measurements. Most studies in coastal and inland waters have compared remote observations to other types of optical data such as the Secchi disk depth and turbidity units (Khorram, 1985; Lathrop and Lillesand, 1986). In oceanic waters, Austin and Petzold (1981) found an empirical relationship between Coastal Zone Color Scanner (CZCS) observations and the diffuse attenuation coefficient for green light at 490 nm. However, because of limitations in the capability of the sensor and the atmospheric corrections, their results are suitable only for waters having an attenuation coefficient of less than 0.5 m^{-1} and a predominance of absorbing material, namely, case I and most case II waters.

Moderately turbid estuaries, those having diffuse attenuation coefficients from 0.5 m^{-1} to about 5 m^{-1}, have optical characteristics determined principally by scattering material, that is, suspended sediment, but with the interaction of multiple constituents, such as humic acids, iron

Address correspondence to R. P. Stumpf, USGS Center for Coastal Geology and Marine Studies, 600 4th Street South, St. Petersburg, FL 33701.

Received 18 October 1990; revised 19 July 1991.

0034-4257/91/$3.50

655 Avenue of the Americas, New York, NY 10010

compounds, and chlorophyll and related pigments. For these waters, which we shall refer to as case III (coastal) waters, following Jerlov's (1976) classification, there is a critical need for information on the attenuation coefficient.

Evaluating changes in the attenuation coefficient in such waters is complicated by the strong spatial and temporal variability that occurs in these environments. Thus, studies often require frequent measurements. This would argue for the use of such data as that collected by the Advanced Very High Resolution Radiometer (AVHRR), which can provide imagery as often as twice daily during the summer.

Our recent demonstration of a physically and statistically strong relationship between water reflectances observed from satellite and the total suspended sediment (or seston) in such waters in Delaware Bay on the Middle Atlantic Bight of the U.S. east coast (Stumpf and Pennock, 1989) leads us to investigate a relationship between water reflectance and the diffuse attenuation coefficient.

THEORY

Above-water irradiant reflectance in vertically homogeneous, optically deep water can be expressed in a form

$$R(\lambda) = Y' \frac{b_b(\lambda)}{a(\lambda) + b_b(\lambda)}, \tag{1}$$

where λ is the wavelength or spectral band, b_b is the backscatter coefficient, a is the absorption coefficient, and Y' (which will be assigned equal to 0.178) is a constant including surface refraction and reflection effects and a constant of proportionality (Gordon et al., 1975). In turbid (case III) water, Eq. (1) can be modified to

$$R(\lambda) = Y' \frac{b^*_{bs}(\lambda)}{s^*(\lambda) + a_x(\lambda)/n_s}, \tag{2}$$

where b^*_{bs} is the specific backscatter coefficient for the sediment (particulates) such that $b_{bs} = b^*_{bs} n_s$; s^* is defined as $b^*_{bs} + a^*_s$, where a^*_s is the specific absorption coefficient for the sediment ($a_s = a^*_s n_s$), a_x is the absorption coefficient for water, chlorophyll-related pigments, and dissolved pigments; and n_s is the sediment concentration (Stumpf and Pennock, 1989).

The diffuse attenuation coefficient K for any wavelength or spectral band is defined as

$$K = \frac{1}{E(z)} \frac{dE(z)}{dz}, \tag{3}$$

where E is the irradiance energy and z is the depth. Establishing a relationship between K and R depends on whether the water is absorption or scattering dominated. In case III waters, K is dependent primarily on the presence of suspended sediment (Biggs et al., 1983; Cloern, 1987), which has a strong backscattering component. We can then characterize K in terms of n_s:

$$K = k^*_s n_s + k_x, \tag{4}$$

where k^*_s is the specific diffuse attenuation coefficient for the suspended sediment or seston and k_x is the diffuse attenuation coefficient for the other constituents (water, chlorophyll, etc.). If we assume that K varies only with k_s ($= k^*_s n_s$) and that $k_x \ll K$, we can substitute (4) into (2) and obtain

$$R(\lambda) = Y' \frac{b^*_{bs}(\lambda)}{s^*(\lambda) + [a_x(\lambda) k^*_s(\lambda)]/K(\lambda)}. \tag{5}$$

Equation (5) can be modified to the logistic equation

$$R(\lambda) = \frac{Y' F^*(\lambda)}{1 + G^*_a(\lambda)/K(\lambda)}, \tag{6}$$

where F^* represents the sediment term (b^*_{bs}/s^*) and G^*_a represents the absorption term of ($a_x k^*_s / s^*$). At long wavelengths where k_w, the attenuation produced by the water, is not negligible, K' ($= K - k_w$) would formally replace K in Eq. (6). However, as k_w at any one wavelength is constant, this modification is not of consequence, except when examining the physical significance of F^* and G^*_a in comparison to values derived from other measurements. This will be discussed later.

We can also examine the role of sediment characteristics in Eq. (6). In Eq. (2), b^*_{bs} and s^* may vary, depending on the surface area, density, and scattering characteristics of the sediments. From Vande Hulst (1957), we can express these variables as

$$b^*_{bs} = b^*_Q n_s / (\rho d), \tag{7}$$

$$s^* = s^*_Q n_s / (\rho d), \tag{8}$$

and

$$k^*_s = k^*_Q n_s / (\rho d), \tag{9}$$

where subscript Q denotes the attenuation efficiency of the type of particle, ρ is the particle density, and d is the particle diameter. Clearly, variations in grain size and optical characteristics of the particles directly alter b^*_{bs}, and also s^* and k^* in the same manner; therefore, some variation in R or K will be expected when comparing them with the sediment concentration [Eq. (2)]. Placing Eqs. (7)–(9) in Eq. (5) results in

$$R(\lambda) = Y' \frac{b^*_Q(\lambda)}{[s^*_Q(\lambda) + a_x(\lambda)k^*_Q(\lambda) / K(\lambda)]}, \quad (10)$$

with the (ρd) terms cancelling. Dividing through by s^*_Q results in Eq. (6) again:

$$R(\lambda) = \frac{Y' F^*_Q(\lambda)}{1 + G^*_{aQ}(\lambda) / K(\lambda)}, \quad (11)$$

where the subscript Q simply denoted that F^* and G^*_a are functions of only optical efficiency terms and not of particle size or density ($F^*_Q = F^*$ and $G^*_{aQ} = G^*_a$).

As the particle size and density term (ρd) drops from the equation in producing Eq. (6), changes in sediment type should have a minor effect on the relationship between K and R. We should expect this result, as both R and K depend primarily on the surface area of the materials, whereas n_s, which is a weight, depends on the volume and density of the material.

We can also examine a solution that does not involve an explicit assumption about the relationship between K and n_s. Philpot (1987) presents a reflectance relationship based on a quasisingle scattering irradiance solution:

$$R(\lambda) = \frac{B_{ss}(\lambda)}{(K\lambda) + K_u(\lambda)}, \quad (12)$$

where K_u is the diffuse attenuation coefficient for upwelling light and B_{ss} is the irradiant backscatter coefficient. Using Philpot's relationships,

$$K_u = aD_u, \quad (13)$$

$$B_{ss} = K - aD_d, \quad (14)$$

where D is the distribution function for upwelling and downwelling light, we have

$$R(\lambda) = \frac{K(\lambda) - a(\lambda)D_d(\lambda)}{K(\lambda) + a(\lambda)D_u(\lambda)} \quad (15)$$

and

$$R(\lambda) = \frac{1 - f_a(\lambda) / K(\lambda)}{1 + g_a(\lambda) / K(\lambda)}, \quad (16)$$

with $f_a = aD_d$ and $g_a = aD_u$. These equations also use K directly and not K'. An equation having the form of Eq. (16) can be derived from Eq. (1) if we assume that K is a linear function of a and b_b such that

$$K = \alpha a + \beta b_b, \quad (17)$$

where α and β are constants of proportionality ($f_a = \alpha a$ and $g_a = \beta a - \alpha a$).

In Eqs. (6) and (16), R will increase with K for fixed a. In case I waters, however, R varies inversely with K (Morel and Prieur, 1977). Conceptually, the difference is straightforward: Where absorbing pigments are important such as most case I, and many case II, waters, increased pigments would increase K but absorb light otherwise available to leave the water column. Where particulates dominate, as in most case III waters (and some case II waters), the increased scattering will increase both K and R. In case III waters, pigments will still have the same effect as for case I waters, namely, increase K and decrease R, but the absorption effect will be less important than that caused by scattering.

METHODS

The processing for reflectance is described in more detail in Stumpf and Pennock (1989) and in Stumpf (1988). Briefly, the above-water reflectance from the satellite is found from

$$R(\lambda) = \pi L_w(\lambda) / E_d(\lambda), \quad (18)$$

where the water-leaving radiance L_w is

$$L_w(\lambda) = [L*(\lambda) - L_A(\lambda)] / T_1(\lambda) \quad (19)$$

the incident radiance on the water's surface, E_d, is approximated by

$$E_d(\lambda) = E_0(\lambda) \cos \theta_0 \; T_0(\lambda), \quad (20)$$

λ being the wavelength or spectral band, E_0 is the solar irradiance at the top of the atmosphere, θ is the solar zenith angle, T_0 is the diffuse transmission from the sun to the surface, including Rayleigh scattering and gaseous absorption, T_1 is the diffuse transmission from the surface to the satellite, $L*$ is the radiance measured at the sensor, and L_A is the atmospheric path radiance. In an area the size of Delaware Bay, the Rayleigh path radiance component of L_A can be treated by a bias correction for the red and near-infrared (near-IR) bands available with the AVHRR

(Stumpf, 1988). The aerosol component is corrected using the radiance over clear water, which has negligible reflectance for red and near-IR light.

The total reflectance R_T for the AVHRR is defined as

$$R_T = \frac{\pi[L_w(1) + L_w(2)]}{E_d(1) + E_d(2)}, \quad (21)$$

where 1 denotes AVHRR Band 1 (red, 580–680 nm) and 2 denotes AVHRR Band 2 (near-infrared, 720–1000 nm). It was previously shown that R_T reduces the effect of chlorophyll-a absorption of red light, while increasing sensitivity over use of the near-infrared band alone (Stumpf and Pennock, 1989). However, use of R_T with the AVHRR requires assumption of an areally uniform atmosphere, which is not a frequent occurrence. To correct for spatial variability, we find a reflectance R_D corrected for aerosol variations at each pixel

$$R_D = R(1) - AR(2). \quad (22)$$

Assigning $A = 1.0$ provides an effective correction for such aerosols as cirrus clouds and for glint. [Other values for A could be found by determining the values of $R(1)$ and $R(2)$ in clearwater, that is, where $R_D = 0$.] R_D is generally proportional to $R(1)$; hence it may be affected by variations in pigments that absorb red light.

The use of the AVHRR has certain advantages in estuarine waters. The near-IR band lies outside the range of effect of most pigments, simplifying some of the absorption problems. The dominant nonchlorophyll pigments, such as the humic acids, iron, and carotenoids, have the greatest effect on shorter wavelengths, especially blue and green; therefore, they will have a greatly reduced [but not always negligible (Witte et al., 1982)] effect on red light. Finally, estuarine case III waters often contain these materials that strongly absorb shorter wavelengths, resulting in the wavelength of maximum light penetration in the water at about 600 nm. This wavelength lies within the bounds of the AVHRR Band 1.

Satellite Data Processing

The AVHRR data sets were obtained as level 1B format digital data (Kidwell, 1986). The scenes were processed to a Mercator projection with a pixel size of 1.18 km at 39°N. To reduce navigation errors in the data, the images were shifted linearly to match the shoreline to within 1 pixel of a digitally overlain database shoreline. Five images from spring of 1987 were used: NOAA-9 from 5 and 6 March, 22 March, and 28 May and NOAA-10 for 30 April.

Valid comparisons of points in the image data to the shipboard stations require relocation of the sampling position to account for tidal motion, as described in Stumpf and Pennock (1989). The median value of the 3×3 block of pixels around each of these relocated points (based on predicted tidal currents) was used for analysis against the shipboard observation.

In situ Methods

In situ observations were made on four cruises (SCENIC-7, -8, -10, -11), corresponding to the dates of the AVHRR imagery. Diffuse attenuation was determined from measurements made with a Biospherical Instruments QSR-100 underwater irradiance meter. This meter provides integrated observations of the photosynthetically active radiation from 400 nm to 700 nm. Measurements were made at 0.25–0.5 m intervals, with deck observations made to assure constancy of the incident light during the measurement period. Based on the solution to (3), namely Beer's law, K was found from linear regression of $\ln [E(z)/E(z_o)]$ against z, where z_o is the uppermost depth of measurement. In all cases evaluated, r^2 was greater than 0.97.

Water samples were taken from Niskin bottles at 0.5–1.0 m below the surface. Profiles with transmissometer and the irradiance measurements showed no variation in the optical characteristics of the water in the upper few meters. Suspended sediment concentrations were determined gravimetrically following filtration onto preweighed 1.0 μm Nucleopore filters and vacuum desiccation. Chlorophyll-a was determined fluorometrically following the method of Strickland and Parsons (1972), using the acid correction for phaeophytin as described by Lorenzen (1967). These and other field measurements are described in Pennock (1985).

RESULTS

Attenuation and seston have a strong linear relationship, indicating that Eq. (4) is appropriate in

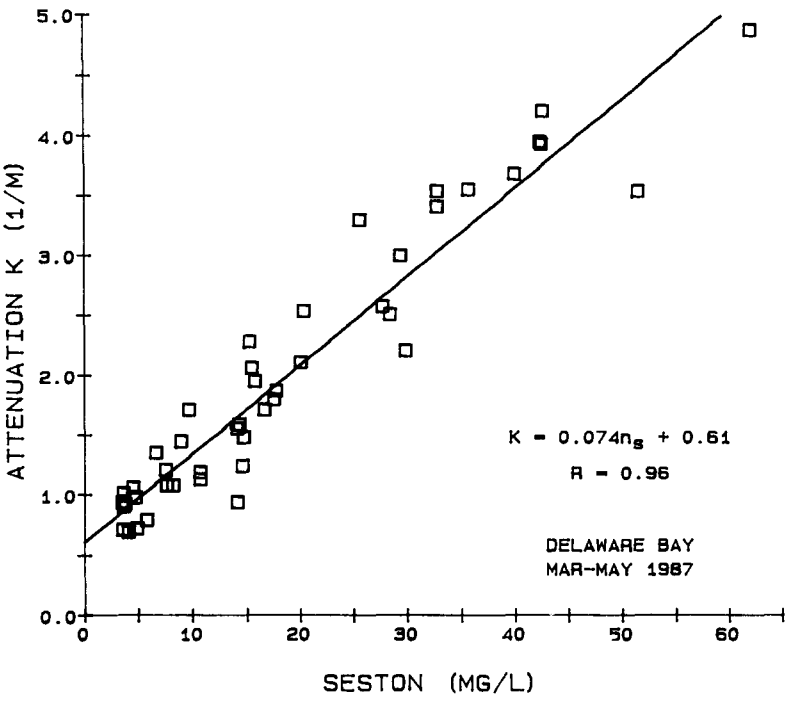

Figure 1. K vs. seston (or total suspended sediments).

lower Delaware Bay (Fig. 1). Although the slope of this relationship is similar to that found in other studies in lower Delaware Bay (Pennock, 1985), the relation could be affected by changes in the size and optical characteristics of the sediment. For example, a different slope applies in the Delaware River turbidity maximum, although the linear relationship still applies (Biggs et al., 1983).

Equation (6) accurately represents the relationship between R_T and K (Fig. 2). When applied to data pairs collected within 3.5 h, over 95% of the variance in the data can be explained by the relationship with a standard error of 0.003 (reflectance units) about the equation solution. Similarly, Eq. (16) also represents the data, showing the same shape as Eq. (6) over the range. Slightly larger errors for points collected further apart in time is expected as a result of spatial

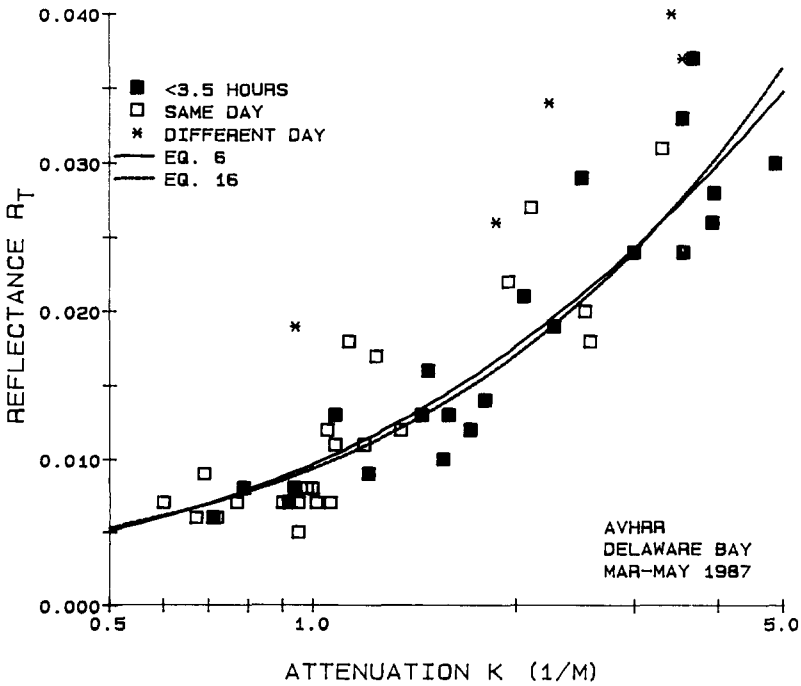

Figure 2. R_T vs. K.

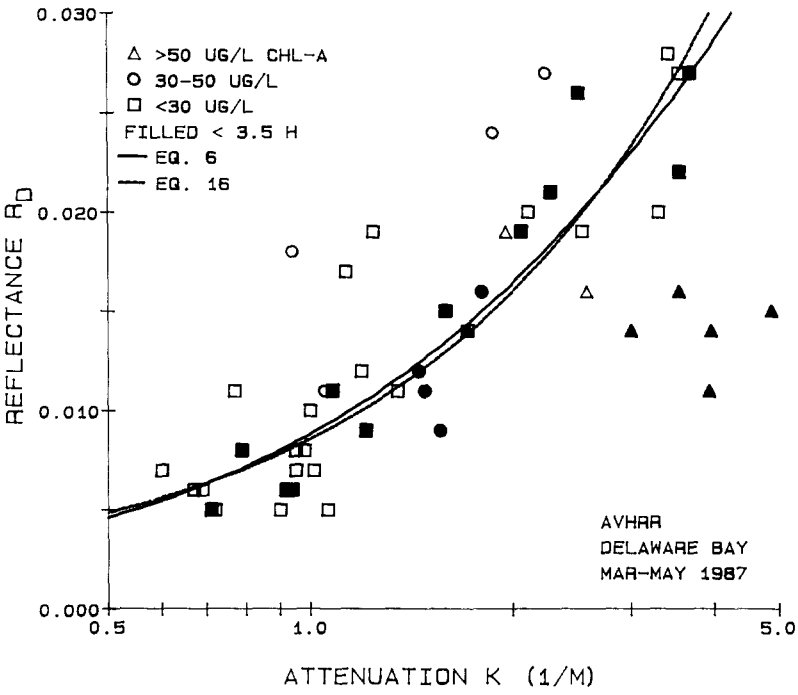

Figure 3. R_D vs. K.

variability and both the tidal and wind-driven excursion (Stumpf and Pennock, 1989). These results suggest that *in situ* and remote observations should be taken within 3 h of each other for valid calibration, even when applying a correction for tidal motion. Without corrections for water movement, lags of less than 1–2 h are preferable.

A plot of R_D vs. K shows a strong relationship of the form of Eqs. (6) and (16) provided that the chlorophyll concentration remains below 50 μg/L (Fig. 3). The absorption produced by high chlorophyll concentrations decreases Band 1 reflectance, thereby decreasing R_D relative to K. Points having chlorophyll concentrations of 30–50 μg L^{-1} tend to lie at or below the curve. Of the five points in this class that lie well above the curve, four consist of satellite and *in situ* observtions taken a day apart; hence less significance should be ascribed to these points. Table 1 shows the coefficients from Eq. (6) for R_T and R_D.

As variability in K tends to increase in proportion to the value of K, the log transform appropriately represents the distribution of the two sets of K (this fact is confirmed by the higher r^2 for the log regression than for the linear regression) (Table 2). When comparing K as estimated from R_T to the *in situ* observations, the results correspond to within 55% at the 95% confidence level (Fig. 4). Similarly, using R_D, the estimated and observed values of K have a 95% confidence interval (C.I.) of 60% when the chlorophyll concentration is <50 μg L^{-1} (Fig. 5).

The scatter in the relationship between observed and calculated K closely matches that found for seston in Stumpf and Pennock (1989). As they described, the discrepancy between ob-

Table 1. Statistics for Eq. (6)

	R_T <3.5 h	R_D $<30\,\mu g\,L^{-1}$ <3.5 h	R_D $<50\,\mu g\,L^{-1}$ <3.5 h	R_T vs. K' $K_W=0.5$ <3.5 h
F^*	0.55 ± 0.23	0.49 ± 0.26	0.63 ± 0.41	0.30 ± 0.06
G_a^*	9.1 ± 5.1	8.2 ± 5.8	11.6 ± 9.1	2.8 ± 0.9
Std. dev.	0.00379	0.00288	0.00279	0.00372
n	22	12	16	22
F-ratio	308	192	243	318

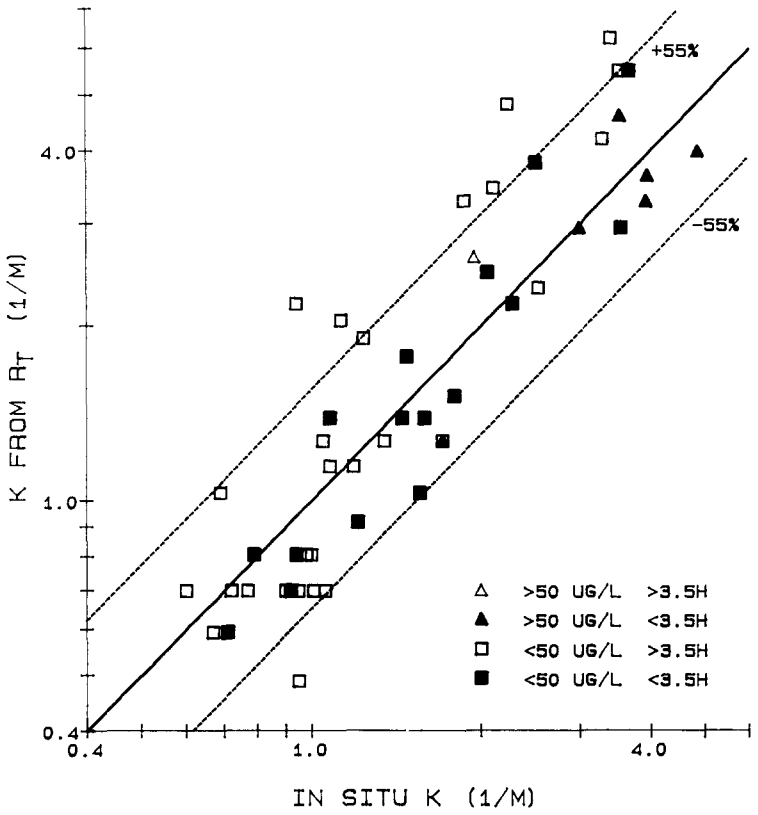

Figure 4. K derived from R_T vs. observed K; dotted line shows the 95% confidence interval of the regression.

served and calculated values results from several factors: errors in the determination of both K (*in situ*) and R; unknown movements or mixing in the water between overpass and sample; and the difference in the scales of the observations. It is not unexpected that movement of the water causes significant discrepancies, even with the correction for tidal motion. Samples taken more than 3.5 h apart show differences of $>60\%$, and those taken on the preceding day can differ by a factor of 2. As other factors, such as wind and high river flow, can produce water movement that

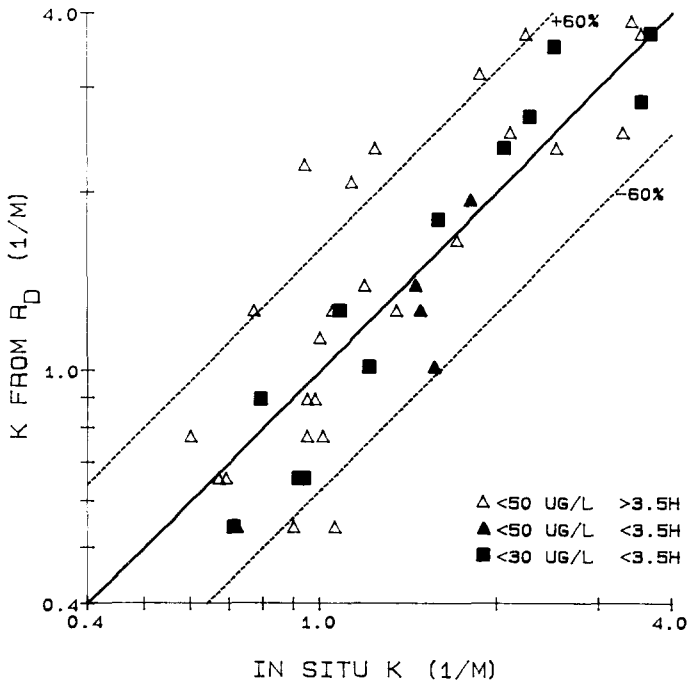

Figure 5. K derived from R_D vs. observed K for chlorophyll-a concentrations less than 50 $\mu g\ L^{-1}$; dotted line shows the 95% confidence interval of the regression.

Table 2. K Estimated from Reflectance vs. K Observed

	$\log_{10} K(R_T)$	$\log_{10} K(R_D)$	$K(R_T)$	$K(R_D)$
Std. dev.	0.0876	0.0965	0.494	0.419
r^2	0.91	0.88	0.87	0.84
F-ratio	210	99	137	76
n	22	16	22	16

cannot be estimated, smaller differences should be obtainable by taking samples within 1–2 h of an overpass.

The difference in scale, however, will remain a source of discrepancy. Reflectance is an average of a 1.2 km^2 area, but K is obtained from measurements in a much smaller parcel of water. Even given ideal atmospheric conditions and perfect measurement and navigation, the difference in sampling area will always produce some discrepancy. Stumpf and Pennock (1989) estimated discrepancies as large as 30% for seston, a significant portion of the total difference. In areas of strong fronts, greater differences may occur.

DISCUSSION

Chlorophyll alters the absorption coefficient; therefore, we can expect additional chlorophyll to increase G_a^* in Eq. (6), which in turn causes R to decrease. This effect is strongest for R_D because this reflectance value behaves like Band 1, which includes chlorophyll absorption bands. In this data set, if G_a^* is increased to 22 m^{-1}, the curve will pass through the group of points in Figure 3 having chlorophyll concentrations greater than 50 μg L^{-1}.

The coefficients derived by substituting K' for K in (6) should be physically meaningful. The results (column 4 of Table 1) are reasonable. As F^* is equivalent to b_{bs}^*/s^* ($\equiv b_{bs}^*/[b_{bs}^* + a_s^*]$), it must be less than 1 (it was found to be 0.30). G_a^* represents the absorption term of $(a_x k_s^*/s^*)$. This should be somewhat greater than the absorption coefficient of water as a_x is somewhat greater than a_w and k_s^*/s^* is slightly greater than one. For the AVHRR, a_w is about 0.3 m^{-1} for Band 1 and greater than 2 m^{-1} for Band 2; hence the observed value of 2.8 m^{-1} is appropriate.

In Eq. (16), the values of the coefficients cannot be meaningfully evaluated. Similar curves can be obtained with substantially different values, particularly for f_a. The similarity between the graphs of Eqs. (6) and (16) is not surprising because (6) can be treated as an approximation to (16) for large values of K. When K becomes much larger than f_a, the numerator in (16) varies little relative to the denominator and can therefore be treated as a constant resulting in an equation of the form of (6).

The relationship between K and n_s (Fig. 1) suggests relatively little variation in the sediment characteristics during the sampling period; thus we could not evaluate the hypothesis that factors such as particle size and density will have a negligible effect on the relation of reflectance and diffuse attenuation [Eqs. (10) and (11)]. If this proves to be the case, then the coefficients in Eq. (6) may apply to a variety of estuaries, particularly when the chlorophyll content remains below 50 μg L^{-1}.

CONCLUSIONS

Equations (6) and (16) provide appropriate representations of the relationship between remotely observed reflectance and observations of the diffuse attenuation coefficient. The coefficients presented here for (6) have applicability to NOAA-9 and NOAA-10 data collected in 1987. The stability of the Band 1 and 2 responses is not quite clear (Abel et al., 1988); if the calibration from digital counts to reflectance varies over time, and cannot be accurately determined, some recalculation of the Eq. (6) coefficients will be necessary for different times.

Further comparison of data from different areas can be used to evaluate the variability in the coefficients of (6). By comparing reflectance or attenuation coefficients with sediment concentration, we could identify areas having sediments with optically significant differences. Thus, these areas could be compared for their relationships between R and K. Equation (6) also has the advantage of being a standard logistic equation and so allows multiple ways of deriving regression solutions.

We would like to thank William Philpot and Ben McPherson for their insightful comments on this manuscript. Initial processing of the satellite data was performed while R. P. Stumpf was with NOAA / NESDIS.

REFERENCES

Abel, P., Smith, G. R., and Levin, R. H. (1988), Results from aircraft measurements over White Sands, New Mexico, to calibrate the visible channels of spacecraft instruments, SPIE, Ocean Optics IX, Orlando, Florida, April 1988, No. 924, 208–214.

Austin, R. W., and Petzold, T. J. (1981), The determination of the diffuse attenuation coefficient of sea water using the coastal zone color scanner, in *Oceanography from Space,* (J. F. R. Gower, Ed.), Plenum, New York, pp. 239–256.

Biggs, R. B., Sharp, J. H., Church, T. M., and Tramantano, J. M. (1983), Optical properties, suspended sediments, and chemistry associated with the turbidity maxima of the Delaware estuary, *J. Can. Fisheries Aquatic Sci.* 40 (*Suppl. 1*):172–179.

Cloern, J. E. (1987), Turbidity as a control of phytoplankton biomass and productivity in estuaries, *Continental Shelf Res.* 7:1367–1381.

Gordon, H. R., Brown, O. B., and Jacobs, M. M. (1975), Computed relationships between the inherent and apparent optical properties of a flat homogeneous ocean, *Appl. Opt.* 14:417–427.

Jerlov, N. G. (1976), *Optical Oceanography,* Elsevier, New York.

Khorram, S. (1985), Development of water quality models applicable throughout the entire San Francisco Bay and Delta, *Photogramm. Eng. Remote Sens.* 51(1):53–62.

Kidwell, K. B. (1986), *NOAA Polar Orbiter Data (TIROS-N, NOAA-6, NOAA-7, NOAA-8, NOAA-9, NOAA-10) Users Guide,* revised January 1988, National Oceanographic and Atmospheric Admin., National Environmental Satellite Data and Information Service, Washington, DC.

Lathrop, R. G., and Lillesand, T. M. (1986), Use of Thematic mapper data to assess water quality in Green Bay and central Lake Michigan, *Photogramm. Eng. Remote Sens.* 52:671–680.

Lorenzen, C. J. (1967), Determination of chlorophyll and pheophytin: spectrophotometric equation, *Limnol. Oceanogr.* 12:343–346.

Morel, A., and Prieur, L. (1977), Analysis of variations in ocean color, *Limnol. Oceanogr.* 22(4):709–722.

Orth, R. J., and Moore, K. A. (1983), Chesapeake Bay: an unprecedented decline in submerged aquatic vegetation, *Science* 222:51–53.

Pennock, J. R. (1985), Chlorophyll distributions in the Delaware Estuary: regulation by light-limitation, *Estuarine, Coastal, Shelf Sci.* 21:711–725.

Pennock, J. R., and Sharp, J. H. (1986), Phytoplankton production in the Delaware estuary: temporal and spatial variability, *Mar. Ecol. Prog. Ser.* 34:143–155.

Philpot, W. D. (1987), Radiative transfer in stratified waters: a single-scattering approximation for irradiance, *Appl. Opt.* 26(19):4123–4132.

Strickland J. D. H, and Parsons T. R. (1972), *A Practical Handbook of Seawater Analysis,* Bulletin Fisheries Research Board of Canada #167, Ottawa, 310 pp.

Stumpf, R. P. (1988), Remote detection of suspended sediment concentrations in estuaries using atmospheric and compositional corrections to AVHRR data, in *Proc. 21st Int. Symposium on Remote Sensing of Environment,* 26-30 October 1987, ERIM, Ann Arbor, MI, pp. 205–222.

Stumpf, R. P., and Pennock, J. R. (1989), Calibration of a general optical equation for remote sensing of suspended sediments in a moderately turbid estuary, *J. Geophys. Res. Oceans* 94(C10):14,363–14,371.

Vande Hulst, H. C. (1957), *Light Scattering by Small Particles,* Wiley, New York.

Witte, W. G., Whitlock, C. H., Harriss, R. C., Usry, J. W., Poole, L. R., Houghton, W. M., Morris, W. D., and Gurganus, E. A. (1982), Influence of dissolved organic materials on turbid water optical properties and remote-sensing reflectance, *J. Geophys. Res.* 87(C1):441–446.